

Direct observation of Al-doping-induced electronic states in the valence band and band gap of ZnO films

Mercedes Gabás*

Dpto. de Física Aplicada I, Lab. de Materiales y Superficies, Universidad de Malaga 29071 Malaga, Spain

Piero Torelli

Laboratorio TASC, IOM-CNR, S.S. 14 km 163.5, Basovizza, I-34149 Trieste, Italy

Nicholas T. Barrett

CEA, IRAMIS/SPCSI/LENSIS, F-91191 Gif-sur-Yvette, France

Maurizio Sacchi

Synchrotron SOLEIL, BP 48, 91192 Gif-sur-Yvette, France and Laboratoire de Chimie Physique-Matière et Rayonnement, UPMC Paris 06, CNRS UMR7614, 11 rue P. et M. Curie, 75005 Paris, France

Fabien Bruneval and Ying Cui

CEA, DEN, Service de Recherches de Métallurgie Physique, F-91191 Gif-sur-Yvette, France

Laura Simonelli

European Synchrotron Radiation Facility, BP 220, 38042 Grenoble, France

Pilar Díaz-Carrasco and José R. Ramos Barrado

Dpto. de Física Aplicada I, Lab. de Materiales y Superficies, Universidad de Malaga 29071 Malaga, Spain

(Received 12 July 2011; revised manuscript received 5 September 2011; published 19 October 2011)

We present a synchrotron radiation hard x-ray photoemission spectroscopy study of the electronic structure of Al-doped ZnO films. Doping-induced states appear between the Zn3*d* and O2*p* levels and in the band gap just below the conduction band minimum (CBM). *Ab initio* calculations confirm the Al impurity origin of these induced states. The drop in the film resistivity with Al doping is not due to the progressive shifting of the Fermi level above the CBM, but rather to the filling of the Al impurity band state, which pins the Fermi level just below the CBM.

DOI: [10.1103/PhysRevB.84.153303](https://doi.org/10.1103/PhysRevB.84.153303)

PACS number(s): 79.60.-i, 71.15.Mb, 73.20.At

Thanks to its excellent properties and low cost,¹ Al-doped ZnO (AZO) is regarded as a promising replacement for indium tin oxide (ITO) as a transparent conductive oxide (TCO) film for photovoltaic and optoelectronic applications.² TCO's play an important role, for example, in the thin film silicon solar cells' global efficiency.³ Front electrodes and back side reflectors must achieve optimum optical and electrical properties, which have to be met by the applied TCO layer. ZnO films doped with group III elements (Al, Ga, In, B) substituted to a Zn atom site were found to have both low resistivity and high transparency,⁴ and thus, they constitute a cheap and nontoxic alternative to ITO. Controlling the Al doping is essential for optimizing solar device performance. However, unambiguous observation of the effect of Al doping on the electronic structure of ZnO and a corresponding, realistic theoretical explanation has, to date, not been provided. The most accepted picture is that donor doping shifts the chemical potential above the bottom of the conduction band (CB),⁵⁻⁷ making conduction carriers available at the Fermi level (FL) while preserving the transparency of the film. Electrical and optical measurements indirectly support this picture,^{8,9} the band gap being measured by optical transitions of the type $p \rightarrow s$. Other theoretical results predict a density of states (DOS) close to the chemical potential due to Al

doping.⁶ Photoluminescence has placed the ionization energy of Al 90 meV below the CB, pinning the FL.¹⁰ In the absence of direct measurement of the effect of realistic Al doping on the electronic states at the FL, it is therefore unclear as to whether the conduction band minimum (CBM) is below or above the chemical potential.

X-ray photoemission spectroscopy (XPS) provides the most direct measure of the DOS, and it was used to investigate the AZO valence band (VB) as a function of Al doping.¹¹ However, due to its high surface sensitivity, standard XPS is not well suited to study the electronic configuration of AZO close to the FL. In fact, the intensity coming from surface-related features (including surface contamination) can mask the bulk contribution. Hard x-ray photoemission spectroscopy (HAXPES), where the contribution of surface features to the total spectrum is strongly reduced,¹² is better suited for the investigation of the bulk states at the FL in AZO. Here, we present HAXPES results for ZnO and AZO films with different Al content, together with *ab initio* and model calculations of the DOS at the VB and FL regions, which conclusively show that Al doping of ZnO leads to impurity bands inside the band-gap region and in the valence band. The position of these bands scarcely changes as a function of doping, thus the FL is pinned. Conductivity changes with Al doping should

therefore be interpreted within the framework of these new results.

We deposited three AZO films and one undoped ZnO film by rf sputtering of ZnO (99.99%) and Al₂O₃ (99.99%) ceramic targets. The temperature of the crystalline Si(100) substrate was 300 °C. Film thicknesses range from 75 nm (undoped film) to 110 nm (highest doping film), as measured by transmission electron microscopy. X-ray-diffraction patterns are very similar for all films and have a single peak at $(34.2 \pm 0.1)^\circ$ with a full width at half maximum $\sim 0.2^\circ$, indicating that the films are highly oriented along the [001] direction and that the ZnO crystal structure is unaffected by low Al doping.¹³ The resistivity is $4.44 \times 10^{-2} \Omega \cdot \text{cm}$ for the undoped film and $2.89 \times 10^{-3} \Omega \cdot \text{cm}$ for the highest doping. Optical transmittance exhibits a sharp ultraviolet absorption edge and a transmittance of about 80% in the visible region. The optical band gap determined from the absorption spectra was 3.21 eV for the undoped film and 3.25 eV for the AZO 2% film. HAXPES experiments were performed at the ID16 beamline of the European Synchrotron Radiation Facility (Grenoble, France) using the VOLPE setup.¹⁴ The photon energy was set to 6995 eV using a Si (220) monochromator; therefore, the measured kinetic energies were greater than 5 keV for all core levels and nearly 7 keV for the VB region. The corresponding probed thickness is ~ 20 nm.¹² The total energy resolution (photon + electron) was 0.35 eV, measured at the FL of a polycrystalline Au foil. Binding energies were referred to this FL. All spectra were recorded at room temperature.

The intensity of the Al 1s peak has been used to determine the relative Al concentration by comparison with the Zn 3s intensity recorded on the same samples and with the same measurement conditions, normalized to the same integration time and corrected for respective cross sections.¹⁵ The Al/Zn ratio in our samples varies from 0.1% to 2%. It is difficult to evaluate an error bar on these values because of the uncertainty in the tabulated subshell cross sections. However, the same analysis using Zn 3p intensities leads to variations of less than 20% in the relative concentrations. The Al concentration of the most heavily doped film has also been estimated using electron dispersive analysis, giving an average Al content of 2% relative to Zn. In the following, we refer to our samples as pure ZnO, AZO 0.1%, AZO 0.7%, and AZO 2%.

Measured valence band spectra are shown in Fig. 1. For clarity the spectra are shifted along the vertical axis. Zn 3d occupancy is not expected to vary upon Al doping; therefore, all spectra were normalized to the same Zn 3d integrated intensity. As doping increases, the gap between the Zn 3d and O 2p levels decreases from 0.75 eV to 0.50 eV [see Fig. 2(a)]. At the same time, an increase in the DOS is observed around 9.1 eV. The inset in Fig. 1 shows that the valence band maximum (VBM) shifts by 0.05–0.1 eV toward the FL, in agreement with previous experimental results.¹¹ Fitting the VBM can be difficult, particularly at low photon energies.¹⁶ Here, the use of hard x-ray minimizes final state effects in the photoemission spectrum and allows reliable extraction of the VBM by linear extrapolation of the VB leading edge. There is also a significant DOS just below the FL, which increases with doping [Fig. 2(b)]. The gap as measured by optical absorption spectroscopy and the experimental VBM places the CBM at

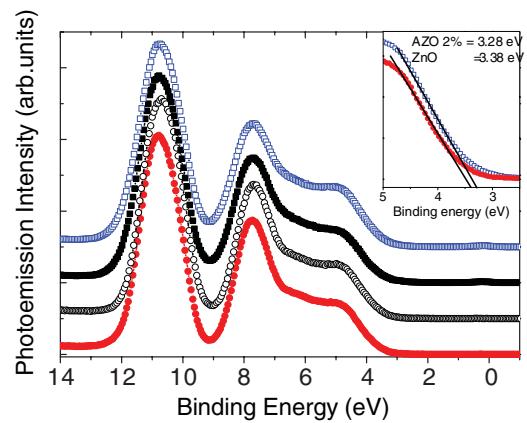


FIG. 1. (Color online) HAXPES VB spectra of the undoped and Al-doped ZnO films. Symbols are as follows: red (dark gray) dots, ZnO; black hollow circles, AZO 0.1%; black full squares, AZO 0.7%; blue (gray) hollow squares, AZO 2%. The inset shows the VBM for the ZnO and the AZO 2%. The VBM maximum values obtained from linear extrapolation are indicated.

the FL. However, the measured DOS is considerably wider than the experimental energy resolution. If only CB states lay below the chemical potential, then progressive filling of the CB with doping should lead to a downward shift of the ZnO VB since the band gap is nearly constant despite doping. This is not at all what we observe. The only possible conclusion is that the DOS observed just below the FL is not the AZO CB but a localized impurity band due to doping. ITO surfaces, for example, were found to exhibit a Fermi edge emission, which was explained by the emission of metallic surface states in the band-gap region.¹⁷

In order to compare and to explain the VB spectra of different films, theoretical simulations of the DOS have been carried out. The *ab initio* calculation using the standard techniques, namely, local density approximation (LDA) or generalized gradient approximation (GGA), fails to account for the band structure of ZnO. There is not only the usual band-gap problem, but also the fact that the calculated valence DOS of ZnO strongly deviates from the experimental measurement. In particular, the Zn 3d is much too shallow, giving rise to an overly strong hybridization with O2p states. The LDA + *U* and GGA + *U* techniques compensate the poor approximations in LDA or GGA with on-site repulsion terms.¹⁸ These techniques are now widely used to perform

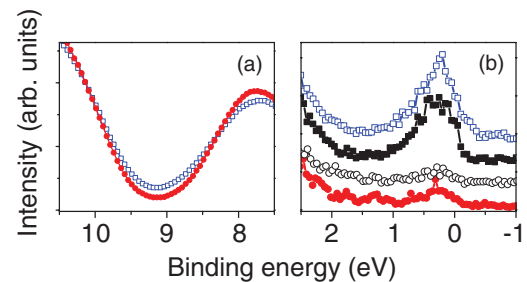


FIG. 2. (Color online) Details of the VB spectra (a) in the gap between the Zn3d and O2p levels, and (b) at the FL region. Symbols and colors are as in Fig. 1.

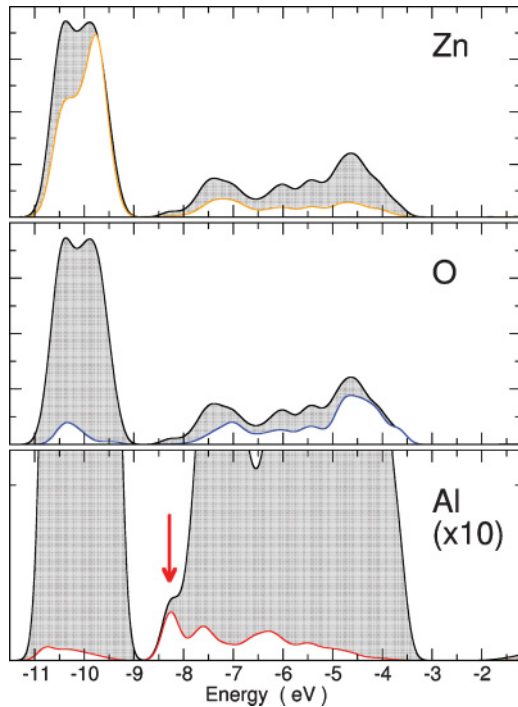


FIG. 3. (Color online) Spherically projected densities of states of AZO with an aluminum content of 4% as obtained from GGA + U calculations. The VBM has been set to the experimental value. The dark areas represent the total DOS and the white areas the projected DOS on Zn (upper panel), on O (middle panel), and in an expanded view on Al (lower panel). The red arrow identifies the Al-related DOS in the gap between the Zn3d and O2p.

improved transition metal oxide calculations. In the present study, our practical goal is to understand where the aluminium states are to be placed in the AZO electronic structure; first of all, we need a realistic DOS for the ZnO host. We therefore employ the GGA + U approach with a term U considered as a parameter whose role is to provide a realistic host DOS. The U value obtained by fitting the experimental ZnO DOS data is 7.5 eV, much higher than the often used 4.5 eV,¹⁹ but in line with several quantum chemistry calculations.^{6,20} The parameter J , of minor importance in GGA + U calculations, was set to 0.75 eV. We used the ABINIT package²¹ for several supercell sizes that account for different Al doping levels (6%: Zn₁₅AlO₁₆, 4.2%: Zn₂₃AlO₂₄, 2.8%: Zn₃₅AlO₃₆, and 1.8%: Zn₅₃AlO₅₄). The binding energy of the Zn3d states within our GGA + U is, by construction, in close agreement with experiment (~ 6.6 eV below the VBM). Using these calculation parameters, a clear valence gap can be observed between the O2p and the Zn3d states. The theoretical spectra have been broadened by the experimental energy resolution. In Fig. 3, we show the projected DOS of an AZO sample on Zn, O, and Al. As the concentration does not influence the conclusions drawn here, we prefer to use a high concentration (4%) for a clearer representation of the data. With respect to undoped ZnO, the Al states affect the VB DOS only very slightly. A remarkable feature is the localization of Al states in the valence gap around 8.3 eV below the experimental FL as shown in Fig. 3 (bottom). The spectral weight is proportional to the Al content according to the calculations and follows precisely the trend we measure

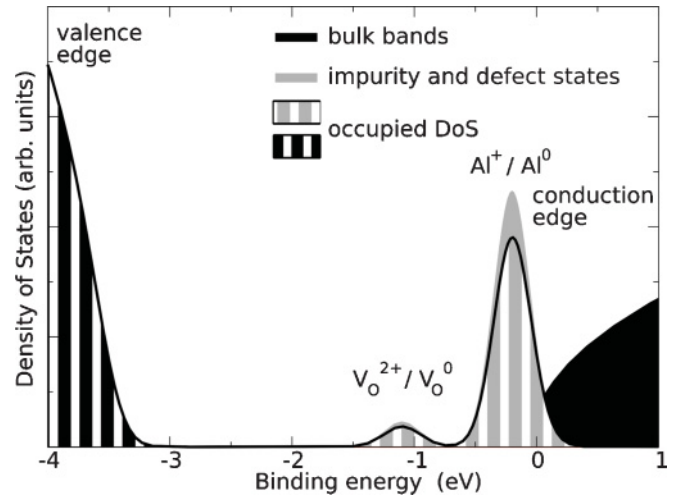


FIG. 4. Density of states assuming 1% Al and 0.05% V_O concentrations. The bulk valence and conduction bands are in black. The defect states (Al and V_O) are in gray. The occupied DOS as measured by HAXPES is symbolized by the white vertical stripes. The DOS are broadened by experimental resolution.

experimentally. This observation explains the difference in the valence band spectra between undoped and 0.1% AZO films, and the 0.7 and 2% AZO films, at about 9 eV below the FL [see Fig. 2(a)].

The HAXPES measures a DOS close to the FL irrespective of film doping [Fig. 2(b)]; however, spectra of the 0.7 and 2% AZO films display a peak 10 times stronger than the undoped and 0.1% films. The strong increase of intensity at the FL upon Al doping indicates a modification of the electronic structure of the AZO films. However, the shape of the structure at FL does not change with the Al concentration. Progressive filling of the bottom of the conduction band by Al doping⁵⁻⁷ would imply broadening of the FL structure with Al content, at variance with our experimental observations. Other experimental data for AZO, however, position differently the states potentially revealed by HAXPES. Photoluminescence places the ionization energy of Al, $\epsilon(\text{Al}^+/\text{Al})$, at ~ 90 meV, below the CBM.¹⁰ The oxygen vacancy (V_O) states [$\epsilon(\text{V}_\text{O}^{2+}/\text{V}_\text{O})$] can be safely placed 1 eV below the CBM.²² Both the donor level of Al and the deep level arising from V_O are introduced into the model. Electron paramagnetic resonance has confirmed the double donor behavior of the V_O.²³ Finally, we add the experimental band gap, the effective masses of the valence and conduction bands, and the experimental energy resolution. Implementing these data into an empirical model based on the Fermi-Dirac distribution gives a full understanding of the experimental results near the FL with the only further assumption being that the impurity band position is independent of the Al concentration. The resulting DOS is depicted in Fig. 4. Significant intensity appears due to electronic states created by Al doping and oxygen vacancies, identifying the nature of the states observed in the FL region. Thus, the drop of more than an order of magnitude in the electrical resistivity is correlated with filling of the Al states near the FL. Other theoretical calculations have also predicted a small enhancement in the PES intensity close to the chemical potential due to Al doping, although they placed the impurity

band inside the CB.⁶ Our experimental results perfectly match the theoretical calculations, and allow identification of the physical origin of the DOS appearing at and just below the FL. Furthermore, the presence of V_O could reasonably explain the extension of the DOS to almost 1.5 eV below the FL.

The FL position scarcely varies with Al concentration. The presence of the $\epsilon(\text{Al}^+/\text{Al})$ state inside the band gap pins the FL, preventing a shift. For instance, with a very high Al concentration, 5%, the calculated FL is only 50 meV above the CBM. Thus, the spectral weight in the the FL region arises mainly from localized oxygen vacancies and Al states and has only a small contribution from the CBM. This also neatly explains why the increase of Al concentration makes the spectral weight higher rather than wider: the weight of the CB in the spectrum remains unchanged, whereas the weight of the Al impurity band increases linearly. The experimental spectral weight due to the V_O also increases with Al concentration, intuitively explained by the fact that heavily doped samples are more likely to have a higher defect concentration.

In conclusion, we have grown highly oriented ZnO and AZO films with Al doping ranging from 0 to 2 cation%. We have investigated the doping-induced changes in the electronic properties of these samples by core level and valence band HAXPES. Al states arise in the VB at about 5 eV below the VBM, most notably for the 0.7 and 2% AZO films. In the FL region, we observe a large increase of the photoemission

intensity for Al content exceeding 0.7%. The onset of a photoemission peak at the FL is accompanied by a strong decrease of the electrical resistivity. Theoretical calculations have helped to provide direct evidence of the character of the near FL states, which can be attributed to oxygen vacancies and Al-induced states. Thus, contrary to what was generally believed, the conductivity in AZO is not due to the FL shifting progressively up above the CBM with increasing Al doping. Rather, it can be explained in terms of filling of the Al impurity band just below the CB edge, which in turn pins the FL. Our experimental results match with photoluminescence and agree with *ab initio* theory and an empirical model, not only in the FL region, but also in the valence band gap, where the Al-derived states predicted by GGA + U calculations are visible. Therefore, we provide a direct proof of the picture which attributes the change of the AZO film resistivity to the appearance of impurity bands in the gap as a function of the Al doping rather than gradual filling of the bottom of the conduction band.

The Spanish Ministerio de Ciencia e Innovación has contributed with research projects TEC2007 60996 and FUNCOAT-CSD2008-00023-CONSOLIDER INGENIO. The computer simulations were performed using HPC resources from GENCI-CINES and GENCI-CCRT (Grant 2011-gen6018). Y. Cui was funded by the CEA materials program.

*mgabas@uma.es

¹S. B. Majumder, M. Jain, P. S. Dobal, and R. S. Katiyar, *Mater. Sci. Eng. B* **103**, 16 (2003).

²T. Minami, *Semicond. Sci. Technol.* **20**, S35 (2005).

³J. Hüpkens, J. Müller, and B. Rech, *Transparent Conductive Zinc Oxide. Basics and Applications in Thin Film Solar Cells*, edited by K. Ellmer, A. Klein, and B. Rech, Springer Series in Materials Science (Springer, Berlin, Heidelberg, New York, 2007).

⁴T. Minami, *MRS Bull.* **25**, 38 (2000).

⁵Y. Imai, A. Watanabe, and I. Shimono, *J. Mat. Sci. Mater. Electron.* **14**, 149 (2003).

⁶P. Palacios, K. Sánchez, and P. Wahnón, *Thin Solid Films* **517**, 2448 (2009).

⁷M. Bazzani, A. Neroni, A. Calzolari, and A. Catellani, *Appl. Phys. Lett.* **98**, 121907 (2011).

⁸K. C. Park, D. Y. Ma, and K. H. Kim, *Thin Solid Films* **305**, 201 (1997).

⁹H. Mondragón-Suarez, A. Maldonado, M. de la L. Olvera, A. Reyes, R. Castanedo-Pérez, G. Torres-Delgado, and R. Asomoza, *Appl. Surf. Sci.* **193**, 52 (2002).

¹⁰H. P. He, H. P. Tang, Z. Z. Ye, L. P. Zhu, B. H. Zhao, L. Wang, and X. H. Li, *Appl. Phys. Lett.* **90**, 023104 (2007).

¹¹M. Gabás, S. Gota, J. R. Ramos-Barrado, M. Sánchez, N. T. Barrett, J. Avila, and M. Sacchi, *Appl. Phys. Lett.* **86**, 042104 (2005).

¹²M. Sacchi, F. Offi, P. Torelli, A. Fondacaro, C. Spezzani, M. Cautero, G. Cautero, S. Huotari, M. Grioni, R. Delaunay, M. Fabrizio, G. Vankó, G. Monaco, G. Paolicelli, G. Stefani, and G. Panaccione, *Phys. Rev. B* **71**, 155117 (2005).

¹³M. Gabás, P. Díaz-Carrasco, F. Agulló-Rueda, P. Herrero, A. R. Landa-Cánovas, and J. R. Ramos-Barrado, *Solar Energy Mater. Solar Cells* **95**, 2327 (2011).

¹⁴P. Torelli, M. Sacchi, G. Cautero, B. Krastanov, P. Lacovig, P. Pittana, R. Sergio, R. Tommasini, A. Fondacaro, F. Offi, G. Paolicelli, G. Stefani, M. Grioni, R. Verbeni, G. Monaco, and G. Panaccione, *Rev. Sci. Instrum.* **76**, 023909 (2005).

¹⁵J. H. Scofield, LLNL Report No. UCRL-51326, 1973 (unpublished).

¹⁶S. A. Chambers, T. Droubay, T. C. Kaspar, M. Gutowski, and M. van Schilfgaarde, *Surf. Sci.* **554**, 81 (2004).

¹⁷Y. Gassenbauer, R. Schafrank, A. Klein, S. Zafeiratos, M. Havecker, A. Knop-Gericke, and R. Schlögl, *Phys. Rev. B* **73**, 245312 (2006).

¹⁸A. I. Liechtenstein, V. I. Anisimov, and J. Zaanen, *Phys. Rev. B* **52**, R5467 (1995).

¹⁹A. Janotti, D. Segev, and C. G. Van de Walle, *Phys. Rev. B* **74**, 045202 (2006).

²⁰A. N. Andriotis, R. M. Sheetz, and M. Menon, *Phys. Rev. B* **81**, 245103 (2010).

²¹X. Gonze *et al.*, *Comput. Phys. Commun.* **180**, 2582 (2009).

²²Y. W. Heo, D. P. Norton, and S. J. Pearton, *J. Appl. Phys.* **98**, 073502 (2005).

²³D. Pfisterer, J. Sann, D. M. Hofmann, B. Meyer, T. Frank, G. Pensl, R. Tena-Zaera, J. Zúñiga-Pérez, C. Martínez-Tomás, and V. Muñoz-Sanjosé, *Phys. Status Solidi C* **3**, 997 (2006).